Science in China Series B: Chemistry

www.scichina.com
chem.scichina.com
www.springerlink.com

Catalytic activity correlation of Ni(II), Co(II) and Pd(II) complexes to metal atom net charge

ZHANG XiongFei[2], DUAN BaoGen[1], SUN WenHua[3], HSU Shaw Ling[2] & YANG XiaoZhen[1†]

[1] State Key Laboratory of Polymer Physics and Chemistry, Center for Molecular Sciences, Institute of Chemistry, Chinese Academy of Sciences, Beijing 100190, China;
[2] Department of Polymer Science and Engineering, University of Massachusetts Amherst, MA 01003, USA;
[3] Key Laboratory of Engineering Plastics and Beijing National Laboratory for Molecular Sciences, Institute of Chemistry, Chinese Academy of Sciences, Beijing 100190, China

The metal atom net charge correlation (MANCC) method was developed in prediction of catalyst activity of asymmetric late-transition metal complexes, 2-quinoxalinyl-6-iminopyridine Ni (II), 2-imino-1, 10-phenanthroline Co(II) and 2-methoxycarbonyl-6-iminopyridine Pd(II) complexes, from the net charge of the metal atom for ethylene polymerization. Dreiding force field was modified according to the X-ray diffraction data. We found that the asymmetric structure of the complexes resulted in a charge difference between two halogen atoms coordinated to the metal atom. In order to remove such contribution we introduced the effective charge Q_{eff}, which was obtained by the charge equilibration (QEq) approach. The results verified the successful introduction of Q_{eff} and showed that the catalytic activities of different complexes are related to central metal atom effective charge.

asymmetric catalyst, effective charge, force field, MANCC, QEq

1 Introduction

Polyolefins are among the most important forms of commercial plastics due to their low cost and versatile properties[1]. The discovery of catalysts for the synthesis of such materials remains a challenging problem[2]. Among the catalysts employed, late-transition metal catalysts are thought to be the most promising ones[3]. There have been enormous efforts on exploiting the late-transition metal catalyst for olefin polymerization[4] since the discovery of highly active Ni(II) and Pd(II) catalysts containing α-diimine ligands by Brookhart and co-workers in 1995[5]. Recent advances in late-transition metal catalysts for olefin polymerization are mainly based on nickel[6], cobalt[7], iron[8] and copper[9].

The influence of ligand on catalytic activity towards ethylene polymerization has been studied by several groups. For example, Olivé[10] concluded that there are four factors affecting the catalyst activity the most: the transition metal-olefin interaction, the metal-alkyl bond stability, the influence of other ligands and substituents attached to the rings, and the steric effect. By studying the influence of central metal atom charge and steric effect on catalytic activity of Zr-based metallocenes, Möhring and Coville[11] pointed out that the electronic effect can contribute as much as 80% of the change in polymerization activity. There are several methods such as *ab initio*[12,13] and density-functional theory (DFT)[14−17] to study the influence of electronic effect of metal atoms on the catalyst performance. The *ab initio* method is an accurate simulation of molecular behavior based on Gaussian program, while the basic notion of DFT is that the energy of an electronic system can be expressed in terms of its density. In most cases, due to

Received March 21, 2008; accepted May 9, 2008; published online November 6, 2008
doi: 10.1007/s11426-008-0112-6
†Corresponding author (email: yangx@iccas.ac.cn)
Supported by the National Natural Science Foundation of China (Grant Nos. 90612015, 20674090, and 20474073), and 973 Project (Grant No. 2004CB720606)

the complex reaction mechanism, it is difficult to determine a good starting point of the catalyst molecules to search the transition state. So in both methods, a huge amount of transit-guided Quasi-Newton (STQN) calculations has to be calculated for seeking the transition state of the polymerization, which is too demanding to be carried out in general laboratories, especially for large catalyst molecules.

It was observed by our group that early-transition metallocene catalyst activity increased with decreasing metal atom charge[18,19]. For late-transition metals such as Ni- and Fe- based catalyst complexes, we found the catalytic activity was also correlated to metal atom charge[20−22]. Based on these observations, we hypothesized that the metal atom charge is most important in terms of affecting late-transition metal-based catalyst performance. Consequently, we developed an empirical method named the metal atom net charge correlation (MANCC) to relate the catalytic activity and the net charge[21, 22]. MANCC method consists of a classical and the empirical method, that is, molecular mechanics (MM) and the charge equilibration (QEq). By using this correlation method, catalytic activity can be semi-quantitatively predicted as long as the net charge of the central metal atom in the catalyst is obtained. When MANCC method is used to predict catalytic activity, the key point to provide accurate catalytic activity result is to set up an appropriate force field for the catalyst molecule, which is not difficult as long as X-ray diffraction data of the catalyst molecule are obtained. In addition, a large amount of time can be saved by using QEq approach to obtain metal atom charge. In this sense, it is both time-saving and accurate to use MANCC method to simulate large catalyst molecule behavior.

Ethylene polymerization mechanism includes the precoordination of the monomer to a free site of the active catalyst, followed by a simple alkyl migration to the monomer to form the new carbon-carbon bond[23,24]. MANCC method has been successfully applied to symmetric catalyst that has two equivalent sites for ethylene to coordinate with. However, the asymmetric catalyst complexes recently drew more attention in the olefin catalyst area[22,25,26], and has no C_2 symmetry axis as shown in Figure 1. The asymmetric structure results in different net charges on the two halogen atoms. In this case, if we want to extend MANCC method to predict catalyst activity of the asymmetry complexes containing two halogen atoms, further investigation is needed.

In the present study, we extended MANCC method for 2-quinoxalinyl-6-iminopyridines Ni (II), 2-imino-1, 10-phenanthroline Co(II) and 2-methoxycarbonyl-6-iminopyridine Pd(II) asymmetric catalyst complexes. A new concept named effective charge Q_{eff} is introduced in this paper for the first time to modify MANCC method, in which the electronic difference between two halogen atoms attached to the central metal atom was taken into consideration. The net charge of central metal atom was given by Materials Studio software with QEq and Dreiding force field. The catalytic activity was obtained from published results[26−28]. Then the relationship between effective charge and catalytic activity was obtained. The purpose of this research is to provide a thorough knowledge of late-transition metal catalyst complexes used for olefin polymerization, which is potentially useful for catalyst design.

2 Methods

Figure 1 presents the structures of catalyst complexes **1**—**6**, 2-quinoxalinyl-6-iminopyridines Ni (II). Different complexes differ in substituent R groups and halogen atoms attached to the Ni atom.

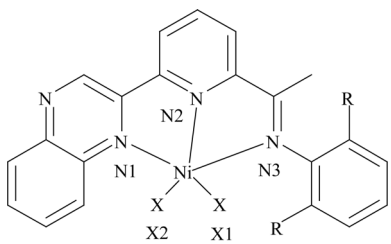

	1	**2**	**3**	**4**	**5**	**6**
R	Me	Et	*i*-Pr	Me	Et	*i*-Pr
X	Cl	Cl	Cl	Br	Br	Br

Figure 1 2-Quinoxalinyl-6-iminopyridines Ni (II) complexes **1**—**6**.

The structures of catalyst complexes **7**—**15** and **16**—**20** are shown in Figures 2 and 3, respectively.

Molecular models were built up by Materials Studio software (version 3.1) as explained below. Dreiding force field was employed here due to its capability of providing accurate geometries for a large number of molecules with parameters deliberately restricted to very

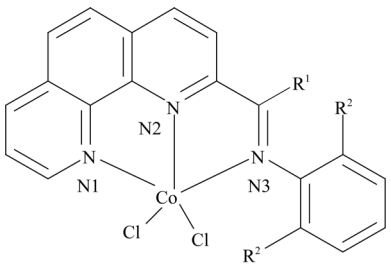

	7	8	9	10	11	12	13	14	15
R^1	H	H	H	Me	Me	Me	Ph	Ph	Ph
R^2	Me	Et	*i*-Pr	Me	Et	*i*-Pr	Me	Et	*i*-Pr

Figure 2 2-Imino-1,10-phenanthroline Co(II) complexes **7**—**15.**

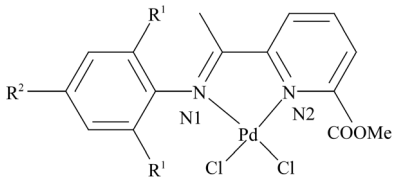

	16	17	18	19	20
R^1	Me	Et	F	Cl	Br
R^2	H	H	H	H	Me

Figure 3 2-Methoxycarbonyl-6-iminopyridine Pd(II) complexes **16**—**20**.

simple rules[29]. The coordinated Ni, Co and Pd parameters were not included in Dreiding force field, so that modification has to be made on the field. The modification of Dreiding force field for all the complexes followed the same way. For example, for complexes **1**—**6**, new type named Ni5+2 was added, which shared the same parameters with metal Ni. For bond stretch and angle bend, harmonic function type and cosine-harmonic function type were chosen as follows, respectively:

$$E_{\text{bond stretch}} = \frac{1}{2} \times K_r (r - r_0)^2,$$

where K_r is the force constant, r is the bond length and r_0 is the equilibrated bond length.

$$E_{\text{angle bend}} = \frac{1}{2} \times K_\theta (\theta - \theta_0)^2,$$

where K_θ is the force constant, θ is the bond angle and θ_0 is the equilibrated bond angle.

The modified parameters for bond stretch and angle bend of Ni(II) complexes are listed in Tables 1 and 2, respectively. For the sake of simplicity, only 4 of the 6 complexes are listed in the tables.

Table 1 Selected bond stretch parameters for complexes **1**, **3**, **5** and **6**

Bond stretch	K_r	R_0 (Å) **1**	R_0 (Å) **3**	R_0 (Å) **5**	R_0 (Å) **6**
Ni5+2-N_Rx	700.0000	2.134	2.176	2.189	2.179
Ni5+2-N_Ry	700.0000	1.945	1.968	1.973	1.965
Ni5+2-N_2	700.0000	2.163	2.147	2.135	2.162
Ni5+2-X	700.0000	2.2206	2.2802	2.3675	2.4255
Ni5+2-X_	700.0000	2.3014	2.2427	2.3996	2.3733
N_Rx-C_R	1050.0000	1.3400	1.3400	1.3400	1.3400
N_Ry-C_R	1050.0000	1.3400	1.3400	1.3400	1.3400

Table 2 Selected angle bend parameters for complexes **1**, **3**, **5** and **6**

Angle bend	K_θ	θ_0 (°) **1**	θ_0 (°) **3**	θ_0 (°) **5**	θ_0 (°) **6**
N_Rx-Ni-N_Ry	100.0000	74.55	72.40	71.88	72.33
N_Rx-Ni-N_2	100.0000	151.51	154.55	153.42	154.53
N_Ry-Ni-N_2	100.0000	77.20	77.53	76.99	77.71
N_Rx-Ni-X	100.0000	92.84	86.35	102.42	85.91
N_Rx-Ni-X_	100.0000	90.44	99.55	90.20	99.76
N_Ry-Ni-X	100.0000	128.13	99.09	142.68	98.11
N_Ry-Ni-X_	100.0000	102.23	136.63	100.50	137.76
N_2-Ni-X	100.0000	99.36	101.87	100.06	102.60
N_2-Ni-X_	100.0000	98.00	95.63	95.22	95.26
X-Ni-X_	100.0000	129.15	124.08	111.83	123.91

The charge of central metal atom was obtained by the combination of charge distribution and energy optimization. To be specific, the charge of each atom was distributed according to QEq method, followed by the optimization of potential energy of the conformer. And then the two steps were repeated until the charge on each atom remained constant. QEq approach is employed here because of its capability of predicting charges of large molecules based only on geometry and experimental atomic properties. QEq approach allows the charges to respond to changes in the environment and it can be applied to any material[30].

The catalytic activity was obtained from published results, which is listed in Table 3 (**1**—**6** as example).

Table 3 Ethylene oligomerization with complexes **1**—**6**/Et_2AlCl

Complex	Activity [a]	Oligomers distribution (%)	
		C_4	C_6
1	6.9	96.7	3.3
2	6.1	89.6	10.4
3	5.3	85.9	14.1
4	7.4	84.2	15.8
5	6.3	89.1	10.9
6	5.2	97.4	3.6

[a] 10^5 g·mol^{-1}(Ni)·h^{-1}.

3 Results and discussion

3.1 Comparison of MM and X-ray results

Since the parameters for coordinated metal atom are not included in Dreiding force field, we have to modify the force field in order to simulate the structure of the complexes in the present study. The results obtained by MM for complexes **4**—**6** are listed in Table 4, and X-ray data are also included. The largest bond length error is less than 0.01 Å, which is 0.5% of typical bond length. The maximum bond angle error is 5.0°, N1-Ni-N3 angle in complex **4**, which lies within the acceptable angle error range. The average angle errors for each complex are the same, i.e., 2.2°, which indicates that the experimental errors for each molecular model are nearly the same. The similar results were also observed for other complexes, which are not shown here for the sake of simplicity. The comparison proves that the modified Dreiding force field has been successfully applied to simulate the structures of catalyst complexes.

3.2 Asymmetric ligand and asymmetric electron distribution

Ethylene polymerization mechanism is shown in Scheme 1. Complex **1** is chosen to illustrate the mechanism. Due to the asymmetric nature of the ligand, the charges on 2 Cl atoms are not equivalent. They are – 0.545, and – 0.535, respectively. The rate-determining step of ethylene polymerization is the alkyl migration to the monomer, the chain propagation step[31]. For the alkyl group to migrate, the Ni—R bond (the Ni atom to the monomer bond or to the alkyl bond) should have suitable stability. According to Olivé's concept[10], the electron-donating or the electron-withdrawing ligand connected to the metal atom (M) will reduce or increase the positive charge on the metal atom, thus decreasing or increasing the bond stability of M—R. As a result, the M—R bond becomes more active or inactive. Therefore, asymmetric ligand results in different Ni-R bond strength and activities.

3.3 MANCC modification

To successfully predict catalytic activity, it is crucial to obtain the charge on metal atom correctly. Metal atom Q_{CM} is given by QEq, which gives charge results on the basis of molecular geometry. Since the two Ni—X(Cl, Br) bonds in 2-quinoxalinyl-6-iminopyridines Ni (II), which are the free sites for ethylene monomer to coordinate with, are not equivalent, their contributions to metal atom charge are thus not equivalent. Since the net charge

Table 4 Selected bond lengths and angles for complex **4**—**6**

Bond and angle	4		5		6	
	X-ray	MM	X-ray	MM	X-ray	MM
Bond lengths (Å)						
Ni—N1	2.239	2.243	2.219	2.221	2.199	2.193
Ni—N2	1.991	1.994	1.983	1.989	1.975	1.980
Ni—N3	2.128	2.126	2.150	2.155	2.172	2.169
Ni—Br1	2.3095	2.310	2.3675	2.366	2.4255	2.421
Ni—Br2	2.4259	2.424	2.3996	2.397	2.3733	2.374
Bond angles (°)						
N1—Ni—N2	76.43	79.601	76.88	81.141	77.33	81.298
N1—Ni—N3	152.31	155.122	153.42	154.117	154.53	156.381
N2—Ni—N3	76.27	76.589	76.99	75.476	77.71	75.952
N1—Ni—Br1	118.93	113.934	102.42	100.732	85.91	82.944
N1—Ni—Br2	80.64	75.846	90.20	92.007	99.76	98.069
N2—Ni—Br1	147.68	145.896	147.68	150.726	98.11	95.255
N2—Ni—Br2	100.50	100.331	100.50	98.075	137.76	140.769
N3—Ni—Br1	91.52	91.058	97.06	94.449	102.60	105.197
N3—Ni—Br2	103.18	101.380	99.22	102.025	95.26	95.573
Br1—Ni—Br2	111.83	113.330	111.83	110.981	123.91	123.749

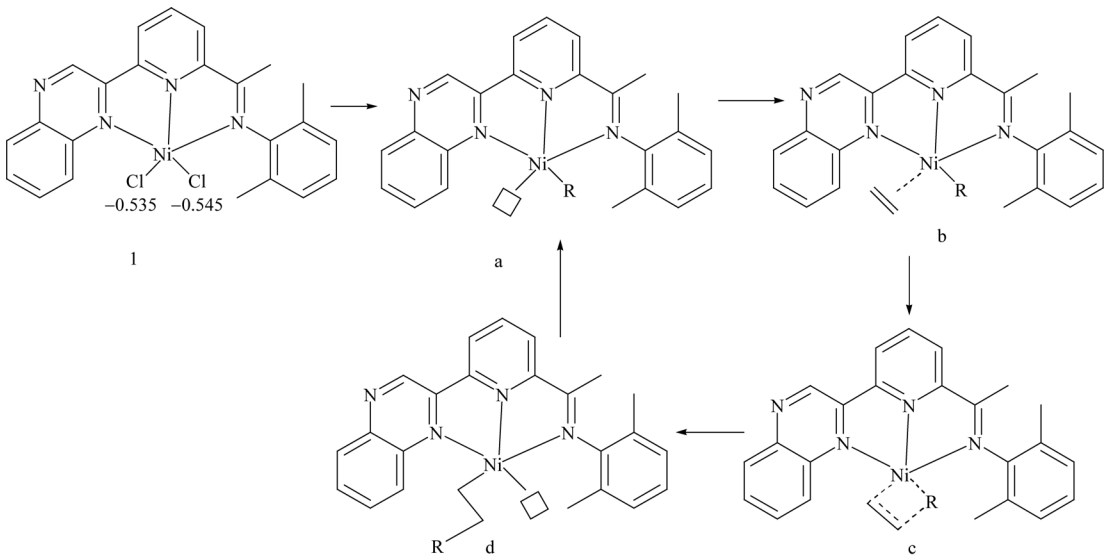

Scheme 1 Mechanism of ethylene polymerization.

of the central metal atom is influenced by molecular orbital hybridization of the complex, the asymmetric ligand structure results in different M—R bonds as indicated by the charge difference ΔQ on the two chlorine atoms. Therefore, the net charge on the metal atom Q_{CM} is not only for tuning the stability of the two M—R bonds but also for the asymmetry. It appears that effective charge for adjusting the bond stability has to be measured by removing the contribution of the structural asymmetry. That is, $Q_{eff} = Q_{CM} - \Delta Q$. In which Q_{CM} and ΔQ can be obtained by QEq approach. Thus Q_{eff} is the central metal atom net charge excluding the electron effect from two halogen atoms. For symmetric catalyst ΔQ is equal to zero and $Q_{eff} = Q_{CM}$. It is thus concluded that MANCC method has been developed from the symmetric complexes to asymmetric ones. And the structural asymmetry has been included in Q_{eff}.

3.4 Verification of Q_{eff} concept

Relationship between Q_{CM} and Q_{eff} for complexes **1**—**6** is listed in Table 5. When Q_{CM} is used to characterize the central metal atom net charge, it is easy to find the Q_{CM} changes in the order of 0.433 (**4**) < 0.443 (**5**), which contradicts the fact that the electron donating ability of methyl group in **4** is weaker than that of ethyl group in **5**. However, Q_{eff} changes in the following order: 0.479 (**1**) > 0.469 (**2**) > 0.429 (**3**); 0.413 (**4**) > 0.394 (**5**) > 0.385 (**6**), which is in accordance with the sequence that the electron donating ability increases from methyl to isopropyl groups. It is concluded that effective charge is successful in modifying MANCC method to characterize asymmetric catalysts.

The plots of catalytic activity versus Q_{CM} and Q_{eff} are shown in Figures 4 and 5, respectively. In both plots, the catalytic activity increases with metal charge, regardless of the halogen species. Complexes **1**—**3** have higher net charge than complexes **4**—**6**, due to the higher electron withdrawing ability of Cl than Br. In Figure 4, spots are widely spread especially for the complexes containing

Table 5 Relationship between nickel atom net charge and effective charge

No.	**1**	**2**	**3**	**4**	**5**	**6**
Q_{CM}	0.489	0.482	0.458	0.433	0.443	0.406
Q_{eff}	0.479	0.469	0.429	0.413	0.394	0.385

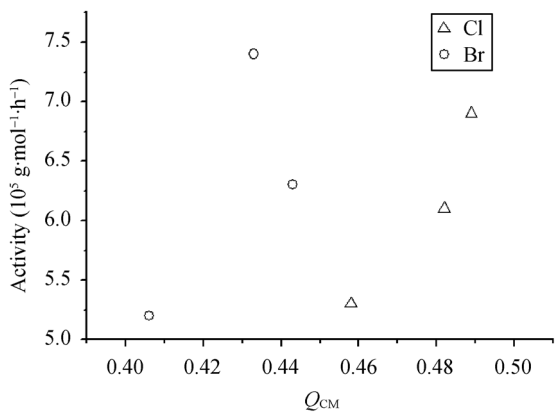

Figure 4 Catalytic activity vs. Q_{CM} for complexes **1**—**6**.

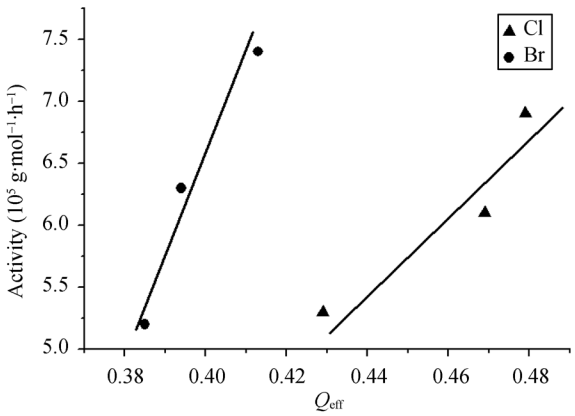

Figure 5 Catalytic activity vs. Q_{eff} for complexes **1**—**6**.

Br atom. However, the spots have a more linear relationship for complexes **1**—**3** and **4**—**6** in Figure 5. The plots demonstrate the accuracy of using Q_{eff} to correlate catalytic activity.

3.5 Correlation between catalytic activity and Q_{eff} for Ni(II), Co(II) and Pd(II) complexes

In our previous study, it was found that catalytic activity of early-transition metal complexes (Ti and Zr metallocenes) increases with the decreasing net charge on metal atom[18,19], which is in agreement with Olivé's concept. In addition, the 4-coordinated salicylaldiminato Ni(II) complex and α-diimino Ni(II) complexes showed an increasing trend in catalytic activity with metal atom charge in the charge range of 0.244—0.264[21]. The different relationships between catalytic activity and metal atom charge for those early-transition and late-transition metal catalyst complexes are due to different *d*-orbital configurations. Ti and Zr hold $3d^2$ configuration while Ni holds $3d^8$ configuration. Ni is electron-rich compared with Ti or Zr. So the Ti—R or Zr—R bond is considered to be stable and Ni—R bond is considered to be already too unstable for ethylene to coordinate with. Both M—R bonds have to reach a suitable stability to get high catalytic activity. For Ni—R bond, the better electron donating ligand results in lower metal atom charge and excessive unstability of Ni—R bond, thus reducing catalytic activity, which is the reason why Ni-based complexes had an increasing trend in catalytic activity with the increasing metal atom charge.

In the present study, 5-coordinated 2-quinoxalinyl-6-iminopyridine Ni(II) catalyst system also showed an increasing trend in catalytic activity with the increasing metal atom charge, which can be seen from Figure 5. The reason can also be attributed to the rich electron effect in Ni atom.

The relationship between catalytic activity and Q_{eff} for complexes **7**—**15** is shown in Figure 6. It is obviously observed that catalytic activity of these 9 complexes decreases with the increasing effective charge for each series of catalysts, which agrees with Olivé's concept. The relationship curve for complexes **13**—**15** has the highest slope within the three curves. So it is safe to draw the conclusion that the electron donating ability of R^1 group affects how fast the catalytic activity decreases with decreasing effective charge. Furthermore, it can be seen from Figure 6 that the catalytic activities of complexes **13**—**15** are higher than those of complexes **7**—**12**. These three series of complexes differ in R^1 substituents. The conjugation effect of phenyl group in complexes **13**—**15** stabilizes the charge on Co atom, which makes Co-Cl bond easier to break. So that the catalytic activities of these three complexes are higher than those of complexes **7**—**12**.

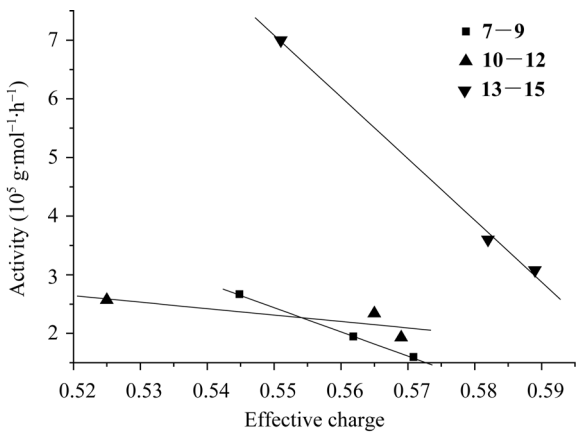

Figure 6 Catalytic activity versus metal atom charge for 2-imino-1, 10-phenanthroline Co(II) complexes.

The catalytic activity of complexes **16**—**20** increases with increasing metal atom effective charge, as shown in Figure 7. The R^1 groups in complexes **18**—**20** are F, Cl and Br, respectively. Compared to the alkyl groups in complexes **16** and **17**, the stronger electron withdrawn ability of R^1 group corresponds to the higher charge on central metal atom. Pd lies within the same group as Ni does, and Pd(II) complexes have the similar relationship between catalytic activity and Q_{eff} as Ni(II)

complexes do, which can be attributed to the similar reason. Based on Figure 7, it can be concluded that electron withdrawn ability results in higher catalytic activity for Pd-based catalyst complexes in the charge range of 0.505－0.584.

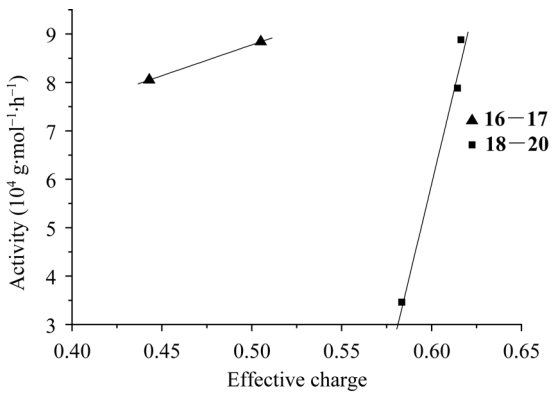

Figure 7 Catalytic activity versus metal atom charge for 2-methoxycarbonyl-6-iminopyridine Pd(II) complexes.

4 Conclusion

Dreiding force field was modified to contain coordinated metal atom and successfully used to simulate Ni(II), Co(II) and Pd(II) catalyst complexes. Then QEq was used to examine the net charge on the central metal atom of the complexes. Because of asymmetry of the complexes, asymmetric electronic structure was formed. In order to remove the asymmetric contribution from the charge of the metal atom, we introduced effective charge concept Q_{eff}, excluding the charge difference ΔQ of the two halogen atoms, to modify the MANCC method. The modified MANCC method is successfully extended to asymmetric catalysts. The catalytic activity increases with increasing Q_{eff} for 2-quinoxalinyl-6-iminopyridines Ni (II) and 2-methoxycarbonyl-6-iminopyridine Pd(II) complexes. While the activity increases with decreasing Q_{eff} for 2-imino-1,10-phenanthroline Co(II) complexes. The difference in variation trend is due to the different electronic configurations.

1 Bateman S A, Wu D Y. Sulfonyl azides——An alternative route to polyolefin modification. J Appl Polym Sci, 2002, 84: 1395－1402[DOI]
2 Odian G. Principles of Polymerization. Wiley: New York, 1991. 630
3 Boffa L S, Novak B M. Copolymerization of polar monomers with olefins using transition-metal complexes. Chem Rev, 2000, 100: 1479－1494[DOI]
4 Ittel S D, Johnson L K, Brookhart M. Late-metal catalysts for ethylene homo- and copolymerization. Chem Rev, 2000, 100: 1169－1204[DOI]
5 Johnson L K, Killian C M, Brookhart M. New Pd(II)- and Ni(II)-based catalysts for polymerization of ethylene and alpha-olefins. J Am Chem Soc, 1995, 117: 6414－6415[DOI]
6 McCord E F, McLain S J, Nelson L T J, Ittel S D, Tempel D, Killian C M, Johnson L K, Brookhart M. ^{13}C NMR Analysis of α-olefin enchainment in poly(α-olefins) produced with nickel and palladium α-diimine catalysts. Macromolecules, 2007, 40: 410－420[DOI]
7 Kissin Y V, Qian C T, Xie G Y, Chen Y F. Multi-center nature of ethylene polymerization catalysts based on 2,6-bis(imino)pyridyl complexes of iron and cobalt. J Polym Sci Part A-Polym Chem, 2006, 44: 6159－6170[DOI]
8 Karam A, Tenia R, Martinez M, Lopez-Linares F, Albano C, Diaz-Barrios A, Sanchez Y, Catari E, Casas E, Pekerar S, Albornoz A. Iron(II) and cobalt(II) tris(2-pyridyl)phosphine and tris(2-pyridyl) amine catalysts for the ethylene polymerization. J Mol Catal A-Chem, 2007, 265: 127－132[DOI]
9 Gibson V C, Tomov A, Wass D F, White A J P, Williams D J. Ethylene polymerisation by a copper catalyst bearing alpha-diimine ligands. J Chem Soc Dalton, 2002, 11: 2261－2262[DOI]
10 Henrici-Olivé G, Olivé S. Influence of ligands on the activity and specificity of soluble transition metal catalysts. Angew Chem Int Ed, 1971, 10: 105－115[DOI]
11 Möhring P C, Coville N J. Quantification of the influence of steric and electronic parameters on the ethylene polymerisation activity of $(CpR)_2ZrCl_2$/ethylaluminoxane Ziegler-Natta catalysts. J Mol Catal, 1992, 77: 41－50[DOI]
12 Cruz V L, Munoz-Escalona A, Martinez-Salazar J. *Ab initio* calculation of ethylene insertion in zirconocene catalyst systems: A comparative study between bridged and unbridged complexes. Polymer, 1996, 37: 1663－1667[DOI]
13 Yoshida T, Koga N, Morokuma K. *Ab initio* theoretical study on ethylene polymerization with homogeneous silylene-bridged group 4 metallocene catalysts: Ethylene insertion and beta-elimination. Organometallics, 1995, 14, 746－758[DOI]
14 Fusco R, Longo L, Masi F, Garbassi F. Olefin polymerization with homogeneous Ziegler-Natta catalysts: A DFT quantum-mechanical study of the reactions of Cp_2MtCH_3Cl complexes (Mt = Ti, Zr) with $Al(CH_3)_3$ and MAO. Macromolecules, 1997, 30: 7673－7685[DOI]
15 Goldstein E, Beno B, Houk K N. Density functional theory prediction of the relative energies and isotope effects for the concerted and stepwise mechanisms of the Diels-Alder reaction of butadiene and ethylene. J Am Chem Soc, 1996, 118: 6036－6043[DOI]
16 Ziegler T. Approximate density functional theory as a practical tool in molecular energetics and dynamics. Chem Rev, 1991, 91: 651－667[DOI]
17 Wang Y, Huang Y H, Liu R Z. Squeezing carbon dimers into the

smallest fullerenes: DFT prediction of new carbon clusters containing double hypercoordinate carbons. J Mol Struc-Theochem, 2006, 775: 61－65[DOI]
18 Guo D W, Yang X Z, Yang L, Li Y F, Liu T Q, Hong H, Hu Y L. Molecular modeling on the prediction of silolene-bridged indenyl metallocene catalysts for isotactic polypropylene. J Polym Sci Part A: Polym Chem, 2000, 38: 2232－2238[DOI]
19 Guo D W, Yang X Z, Liu T Q, Hu Y L. Study on the activity of constrained geometry metallocenes. Macromol Theory Simul, 2001, 10: 75－78[DOI]
20 Guo D W, Han L Q, Zhang T Z, Sun W H, Li T, Yang X Z. Temperature dependence of the activity of a late transition metal catalyst by molecular modeling. Macromol Theory Simul, 2002, 11: 1006－1012[DOI]
21 Zhang T Z, Guo D W, Jie S Y, Sun W H, Li T, Yang X Z. Influence of electronic effect on catalytic activity of salicylaldiminato nickel(II) complexes. J Polym Sci Part A: Polym Chem, 2004, 42: 4765－4774[DOI]
22 Zhang T Z, Sun W H, Li T, Yang X Z. Influence of electronic effect on catalytic activity of bis(imino)pyridyl Fe(II) and bis(imino)pyrimidyl Fe(II) complexes. J Mol Catal A-Chem, 2004, 218: 119－124[DOI]
23 Cossee P. Ziegler-Natta catalysis I. Mechanism of polymerization of α-olefins with Ziegler-Natta catalysts. J Catal, 1964, 3: 80－88[DOI]
24 Arlman E J, Cossee P. Ziegler-Natta catalysis III. Stereospecific polymerization of propene with the catalyst system $TiCl_3$-$AlEt_3$. J Catal, 1964, 3: 99－104[DOI]
25 Chan M S W, Deng L Q, Ziegler T. Density functional study of neutral salicylaldiminato nickel(II) complexes as olefin polymerization catalysts. Organometallics, 2000, 19: 2741－2750[DOI]
26 Adewuyi S, Li G, Zhang S, Wang W Q, Hao P, Sun W H, Tang N, Yi J J. Nickel(II) complexes chelated by 2-quinoxalinyl-6-iminopyridines: Synthesis, crystal structures and ethylene oligomerization. J Organomet Chem, 2007, 692: 3532－3541[DOI]
27 Jie S Y, Zhang S, Wedeking K, Zhang W, Ma H W, Lu X M, Deng Y, Sun W H. Cobalt(II) complexes bearing 2-imino-1,10-phenanthroline ligands: Synthesis, characterization and ethylene oligomerization. C R Chimie, 2006, 9: 1500－1509
28 Zhang W J, Sun W H, Wu B, Zhang S, Ma H W, Li Y, Chen J T, Hao P. Synthesis of palladium complexes containing 2-methoxycarbonyl-6-iminopyridine ligand and their catalytic behaviors in reaction of ethylene and norbornene. J Organomet Chem, 2006, 691: 4759－4767[DOI]
29 Mayo S L, Olafson B D, Goddard III W A. Dreiding: A generic force field for molecular simulations. J Phys Chem, 1990, 94: 8897－8909[DOI]
30 Rappé A K, Goddard III W A. Charge equilibration for molecular dynamics simulations. J Phys Chem, 1991, 95: 3358－3363[DOI]
31 Zeller A, Strassner T. The mechanism of ethylene polymerization by nickel salicylaldiminato catalysts: Agostic interactions and their kinetic isotope effects. J Organomet Chem, 2006, 691: 4379－4385[DOI]